

Effect of Various Factors for the Electrochemical Adsorption of Polydopamine on TiO₂ Film

Naomu Takahashi, Mikito Kitayama

Department of Life, Environment, and Applied Chemistry, Fukuoka Institute of Technology, Fukuoka, Japan

Email: kitayama@fit.ac.jp

How to cite this paper: Takahashi, N. and Kitayama, M. (2022) Effect of Various Factors for the Electrochemical Adsorption of Polydopamine on TiO₂ Film. *Journal of Materials Science and Chemical Engineering*, 10, 15-29.

<https://doi.org/10.4236/msce.2022.103002>

Received: January 27, 2022

Accepted: March 11, 2022

Published: March 14, 2022

Copyright © 2022 by author(s) and Scientific Research Publishing Inc. This work is licensed under the Creative Commons Attribution International License (CC BY 4.0).

<http://creativecommons.org/licenses/by/4.0/>



Open Access

Abstract

To fabricate polydopamine-sensitized solar cells with improved solar power conversion efficiency, the effects of pH, buffer, adsorption time and electrode potential for the electrochemical oxidation and polymerization of dopamine on TiO₂ film were investigated. The optimum pH was around 7. It was found that the use of a buffer, especially 2-(N-morpholino)ethanesulfonic acid, significantly deteriorated the electrochemical adsorption of polydopamine, and the highest solar power conversion efficiency was obtained without buffer. With increasing adsorption time, the amount of adsorbed polydopamine increased but the solar power conversion efficiency decreased, suggesting the increased resistivity of polydopamine with a larger degree of polymerization. It was suggested that the reversal of electrode potential from positive to negative would be essential for the electrochemical adsorption of polydopamine.

Keywords

Dye-Sensitized Solar Cell, Dopamine, Polydopamine, Electrochemical Adsorption, Buffer

1. Introduction

Recent worldwide trend for decarbonization has been accelerating the replacement from conventional fossil fuel to renewable energy sources, and the demand for more inexpensive photovoltaic (PV) generation. The dye-sensitized solar cells (DSSCs) are one of the candidates for replacing the conventional semiconductor PV devices. Intensive studies in the past few decades [1] increased the solar power conversion efficiencies η of DSSCs up to about 12%, of which energy cost would be comparable to the traditional Si solar cells considering the much lower fabrication costs of DSSCs. Further improvements of η with fewer production costs have been requiring the replacement of Ru complex dyes, since Ru is

the typical rare metal that would limit the future mass production of DSSCs. Thus, alternative organic dyes with comparable or even better η have been explored.

In particular, polymer dyes containing π -conjugated systems are potential materials because of their high molar absorption coefficient, wide spectral region of sunlight and high flexibility, in which the modification of the anchoring group or conjugation length greatly affects light absorption and dye binding properties and ultimately overall photovoltaic performance [2]. The endiol units of catechol derivatives as an anchoring group have a special ability to form significant dye-to-TiO₂ charge transfer complexes through chelation with titanium ions in nanocrystalline TiO₂ cells, resulting in new hybrid properties [3] [4] [5] [6]. Dopamine (DA), 4-(2-aminoethyl) benzene-1,2-diol, commonly known as a neurotransmitter, had been reported to exhibit excellent adhesive properties in *Mytilus edulis* foot proteins of marine mussels [7]. Polydopamine (PDA) is known as a black dye that mimic Melanins, representative biological black pigments, derived from another neurotransmitter, L-3,4-dihydroxyphenylalanine (L-DOPA). PDA prepared by oxidant-induced self-polymerization or electrochemical polymerization of DA shows remarkably strong adhesion to organic and inorganic surfaces due to catechol and imine moieties, enabling surface modification, layer-by-layer assembly and nanocomposite film formation [8] [9].

Recently, PDA-DSSCs were fabricated using two methods, dip-coating (DC) and cyclic voltammetry (CV) in tris(hydroxymethyl) aminomethane (THAM) buffer solution at pH 8.5 in a nitrogen atmosphere, and it was reported that the PDA(DC)-DSSC exhibited $\eta = 1.2\%$ under AM1.5 condition, which performed better than PDA(CV)-DSSC ($\eta = 0.9\%$) [10]. Using the same DC method, photovoltaic characteristics of poly-epinephrine and poly-dopamine dyes were compared, and it was found that the former dye exhibited larger η (0.41%) than the latter dye (0.26%) [11]. However, the conditions for fabricating PDA(CV)-DSSC were not investigated in detail in ref. 10, in which the following particular condition was used, DA concentration (0.03 M), the selection of buffer and its concentration (0.01 M THAM), the selection of electrolyte and its concentration (the mixture of dilute 0.1 M HCl and 0.1 M NaOH for pH adjustment), solution pH (pH 8.5), electrochemical potential and its sweep rate ($-1 - +1$ V vs Ag/AgCl and 10 mV/s), all of which should significantly influence not only the electrochemical oxidation and polymerization of DA but also the adsorption of DA on the TiO₂ thin film that should occur prior to the PDA formation. For example, the zeta potential of DA-adsorbed TiO₂ was reported to be highly positive and to increase with increasing DA concentration even at high pH [12], which suggests that DA molecules in DA aqueous solution would repel against the TiO₂ nanoparticles. Also, phosphate buffer was reported to adsorb strongly on the TiO₂ surface, which inhibited the adsorption of L-DOPA [13]. Similarly, a THAM molecule having three hydroxyl groups and one amino group might strongly adsorb on the TiO₂ surface to inhibit the adsorption of DA molecules. The purpose of this

work is to investigate the optimum conditions, especially pH and buffer, for the electrochemical oxidation and polymerization of DA on TiO₂ film in order to fabricate PDA (CV)-DSSC with improved η .

2. Experimental

2.1. Fabrication of TiO₂ Film

2 mL aqueous solution of acetic acid (pH 3) was added to 6 g of anatase-type TiO₂ nano powder (P25; Nippon Aerosil Co., Ltd.), and the mixture was rigorously pulverized using a mortar and pestle for 15 min until obtaining a uniform suspension. Then, the same acetic acid solution was added 1 mL each, and further mixed until adding the total amount of 8 mL. About 30 min after starting the pulverization, 4 g of polyethylene glycol (molecular weight 20,000) was added and further continued mixing. The resultant suspension was coated on a TCO glass (1 × 1 inch, 1.8 mm thickness, type-VU, AGC Inc., Japan) substrate by a screen-printing machine (Mitani Micronics Co., Ltd., Japan) using a screen with 50 μm thickness. After drying, the coated glasses were fired in an electric furnace at 100°C for 20 min, at 350°C for 40 min, and at 450°C for 60 min. **Figure 1(a)** and **Figure 1(b)** show the surface and cross section, respectively, of TiO₂ thin film thus prepared confirming that it had no cracks, and that its film thickness was about 10 μm .

2.2. Electrochemical Adsorption of PDA

Three kinds of 200 ml aqueous solutions were prepared by dissolving 0.1 M Na₂SO₄ as a supporting electrolyte using no buffer or 0.01 M Tris(hydroxymethyl)aminomethane (THAM) or 0.01 M 2-(N-morpholino)ethanesulfonic acid (MES) in distilled water. The pH of aqueous solutions was adjusted to 4.0, 6.0, 7.0 or 8.5 by adding dilute NaOH or H₂SO₄ solutions. After bubbling N₂ for 1 hr, each aqueous solution was divided into two glass containers connected with each

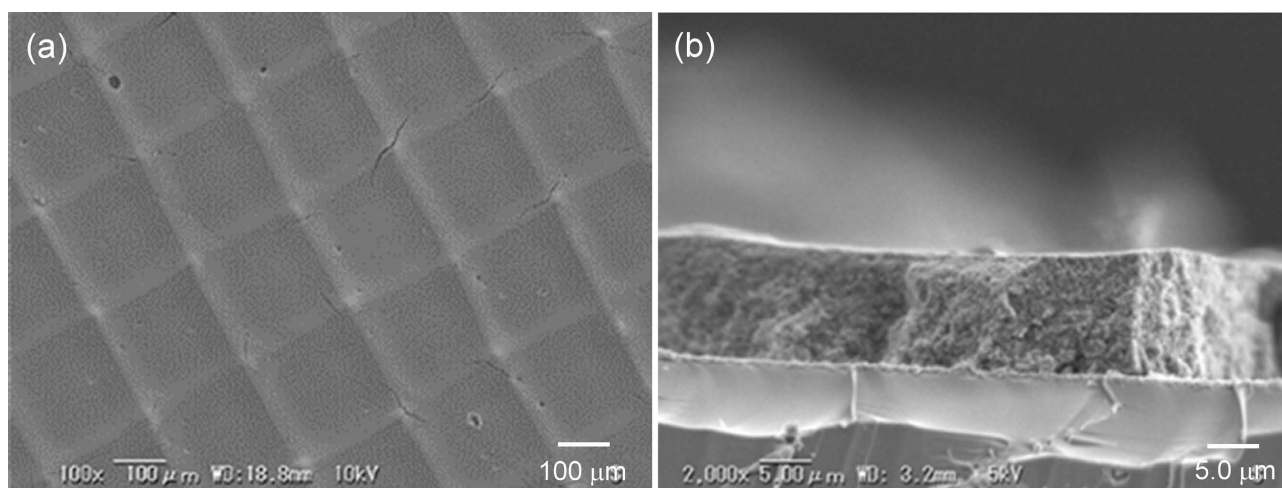


Figure 1. (a) Surface and (b) cross section of TiO₂ thin film, showing that it had almost no cracks, and that its film thickness was about 10 μm .

other by a glass filter. To one container, Dopamine hydrochloride was dissolved to give 0.01 M DA solution, and N₂ bubbling was continued for 30 min. Electro-oxidative polymerization of DA was carried out using a potentiostat (HAB-151A; HOKUTO DENKO Co., Ltd., Japan) linked to a three-electrode system consisting of a counter electrode, a reference electrode and a working electrode. A square Pt plate with dimensions of 1 × 1 inch was immersed as a counter electrode in a glass container without DA, and a TiO₂ film coated TCO glass substrate was immersed as a working electrode in another glass container with DA, in which a Luggin capillary connected to a Ag/AgCl reference (+0.199 V vs. SHE at 25 °C) electrode by a KCl salt bridge was also immersed. The PDA dye was coated on the TiO₂ electrode using cyclic process between 1 V and -1 V vs. Ag/AgCl with a sweep speed of 10 mV/sec while bubbling N₂ for 30 min. All electrochemical measurements were repeated three times to ensure the reproducibility.

2.3. Evaluation of PDA-Coated DSSC

A few drops of 10 mm H₂PtCl₆ 2-propanol solution were put onto a TCO glass substrate. After spreading evenly, the glass substrate was immediately set in a pre-heated furnace at 450 °C, and was fired for 30 min. A plastic film with 25 μm thickness was sandwiched between TiO₂ coated and Pt coated TCO glass substrates as a spacer, and a few drops of I⁻/I₃⁻ electrolyte containing 0.3 M KI and 30 mm I₂ was filled between them to assemble the DSSC. The irradiation area was limited to 1 cm². The DSSC assembly was connected to a potentiostat (HAB-151A; HOKUTO DENKO Co., Ltd., Japan), and its photocurrent density-photovoltage characteristics (I-V curve) were measured under the AM1.5 irradiation using a solar simulator (XES-40S1, SAN-EI ELECTRIC Co., Ltd., Japan). All measurements were repeated three times to ensure the reproducibility.

3. Results and Discussion

3.1. Effect of pH and Buffer (THAM or MES)

Figure 2(a) and **Figure 2(b)** show the cyclic voltammograms (CV curves) of DA obtained at pH 4.0 using THAM and MES, respectively, as a buffer. Both anodic and cathodic currents are very small, and no clear oxidation peak was observed in these figures. **Figure 3(a)** and **Figure 3(b)** show the CV curves of DA obtained at pH 6.0 using THAM and MES, respectively, as a buffer solution. When THAM was used as a buffer, large oxidation peaks were observed at about +0.55 V and +0.75 V vs. Ag/AgCl, the latter which was not observed in the first cycle but appeared in the second cycle onward. The corresponding reduction peak was only observed for the oxidation peak at about +0.7 V vs. Ag/AgCl, suggesting that the electrochemical reaction proceeding at about +0.55 V vs. Ag/AgCl would be an irreversible process, and that at +0.75 V vs. Ag/AgCl would be a reversible process. When MES was used as a buffer, both anodic and cathodic currents were much smaller, and a small oxidation peak was observed only at around +0.55 V vs. Ag/AgCl. **Figure 4(a)** and **Figure 4(b)** show the CV curves of DA

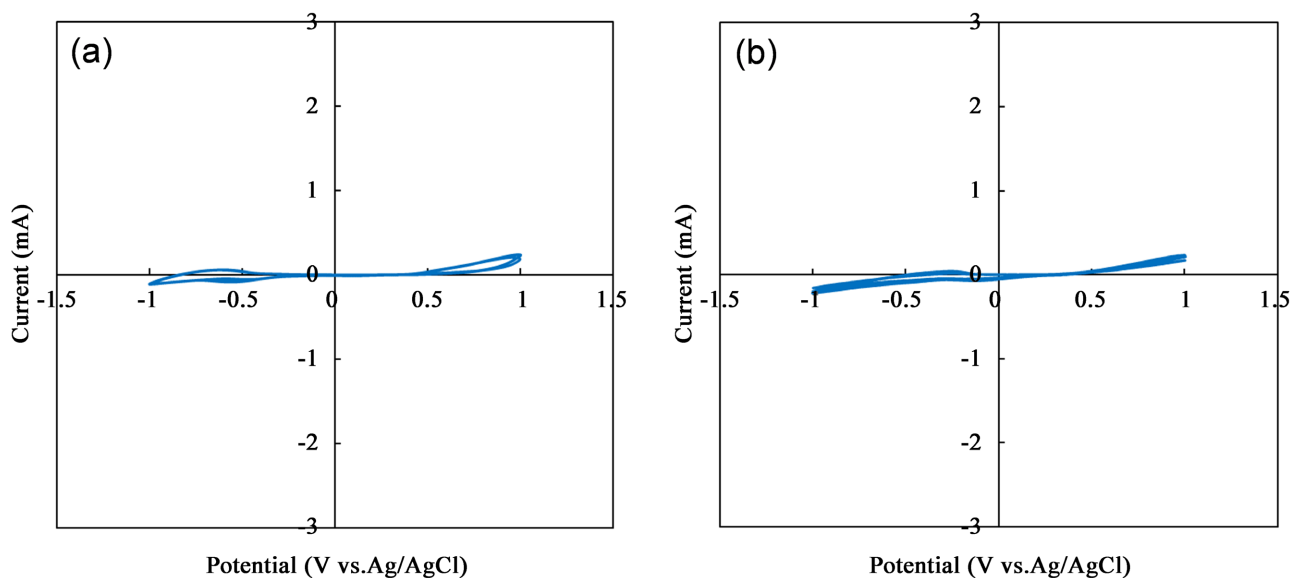


Figure 2. Cyclic voltammograms of DA obtained at pH 4.0 using (a) THAM and (b) MES as a buffer.

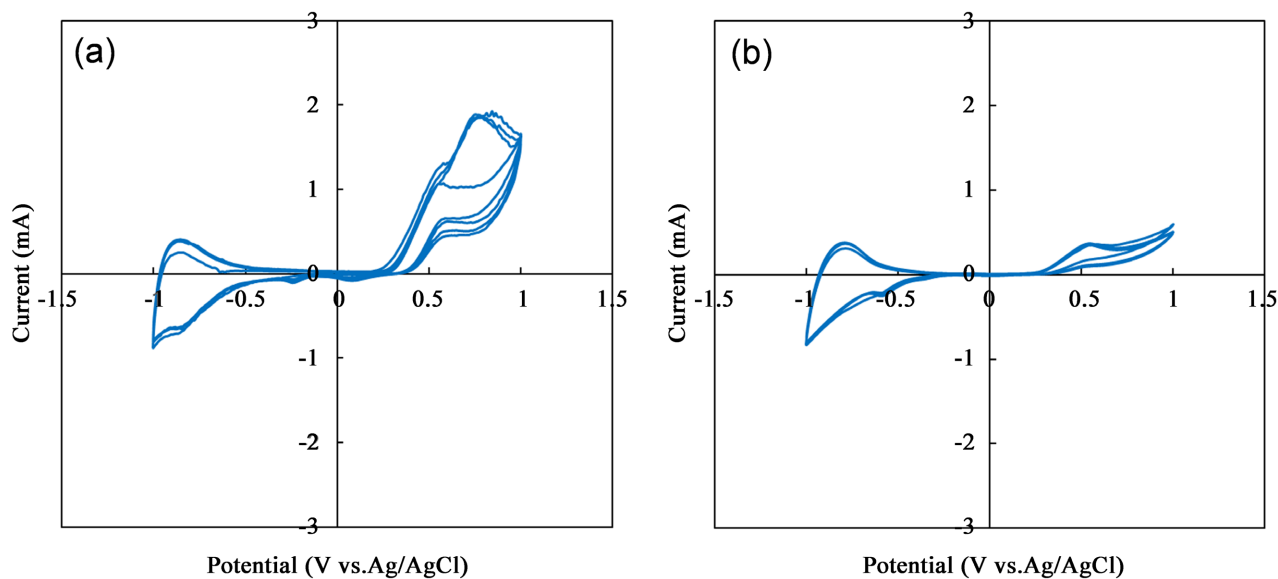


Figure 3. Cyclic voltammograms of DA obtained at pH 6.0 using (a) THAM and (b) MES as a buffer.

obtained at pH 7.0 using THAM and MES, respectively, as a buffer solution. When THAM was used as a buffer, the largest anodic current flowed in this experiment, and an oxidation peak appeared at about +0.75 V vs. Ag/AgCl, and that at about +0.55 V vs. Ag/AgCl was observed only in the first cycle and was not clearly observed in the second cycle onward. When MES was used as a buffer, an oxidation peak at about +0.5 V vs. Ag/AgCl was observed, but was much smaller than that using THAM buffer, and decreased with cycles. In contrast, the reduction peaks at around -0.7 V vs. Ag/AgCl were clearly observed in all cycles. **Figure 5(a)** and **Figure 5(b)** show the CV curves of DA obtained at pH 8.5 using THAM and MES, respectively, as a buffer solution. When THAM was used as a buffer, large oxidation peaks were observed only at about +0.4 V and the corresponding

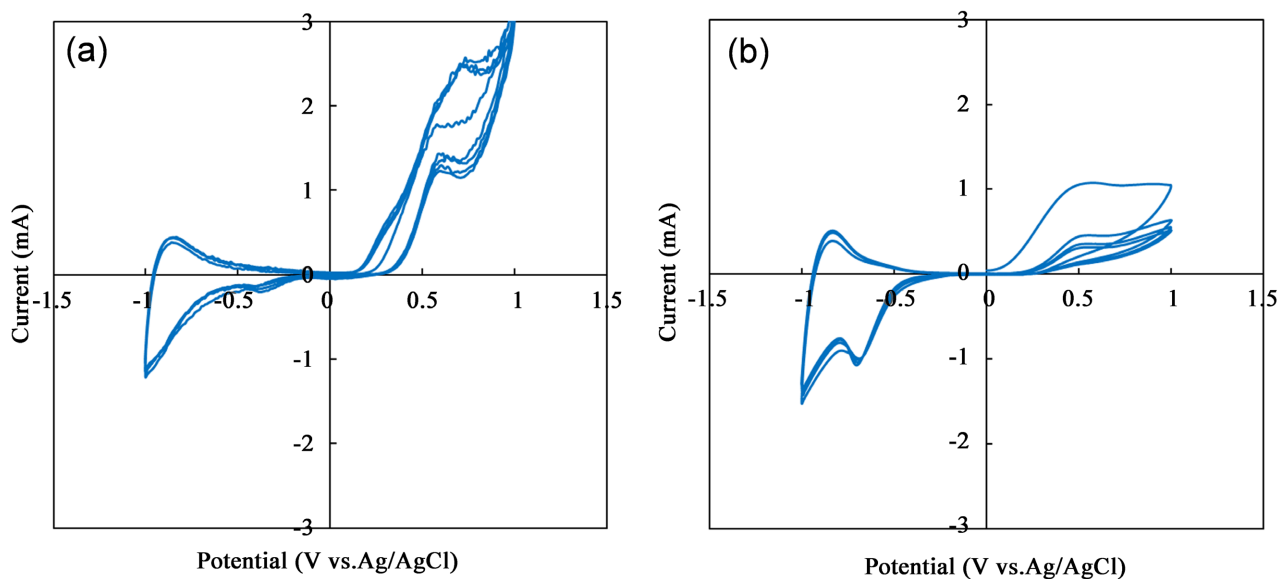


Figure 4. Cyclic voltammograms of DA obtained at pH 7.0 using (a) THAM and (b) MES as a buffer.

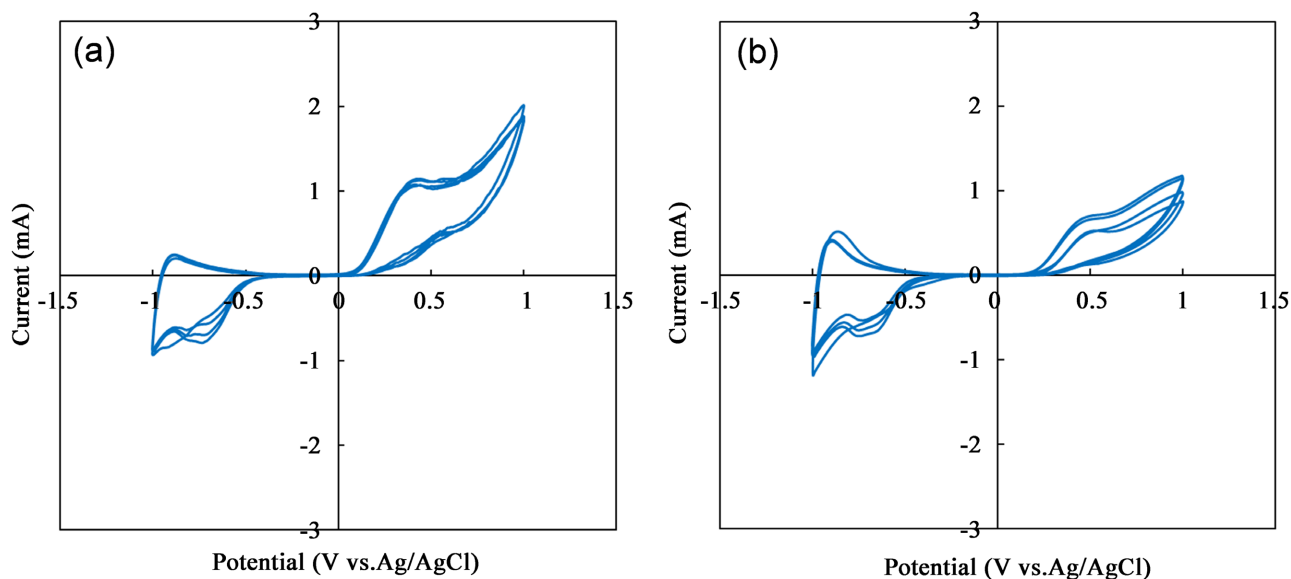
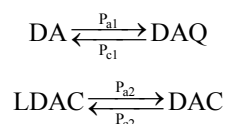


Figure 5. Cyclic voltammograms of DA obtained at pH 8.5 using (a) THAM and (b) MES as a buffer.

reduction peak was not observed. The reduction peaks at around -0.75 V vs. Ag/AgCl were clearly observed in the first and second cycles, which decreased with cycles. When MES was used as a buffer, the oxidation peaks were smaller than that using THAM, but the CV curves were similar to those using THAM. The reason why almost no oxidation of DA occurred in low pH would be due to the positive charge of an amine group in the DA molecule resulting in repelling of DA molecules against the TiO_2 electrode to inhibit their adsorption on TiO_2 surface when the potential of working electrode was positively polarized. Thus, when pH approached neutral, pH 6.0 and 7.0, the number of positively charged DA molecules should decrease, and the neutral DA molecules were able to be adsorbed on the TiO_2 surface to be oxidized. At pH 8.5, the self-polymeri-

zation of DA molecules would proceed [10], and hence, the anodic current of DA would decrease. The reason why the oxidation peaks using MES are much smaller than those using THAM would be explained by the different charging states of these buffers. Because MES with a sulfonyl group having low pK_a should be negatively charged in aqueous solutions in the current experimental condition, MES ions would be strongly attracted to the TiO_2 electrode to inhibit the adsorption of DA molecules on TiO_2 surface when its potential was positively polarized.

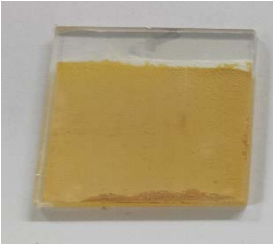
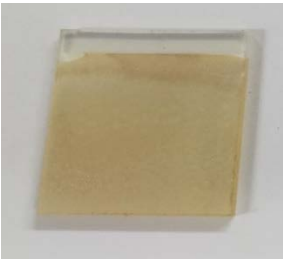
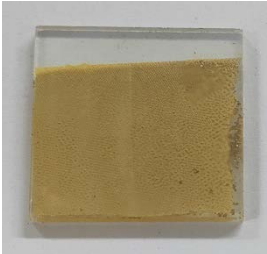
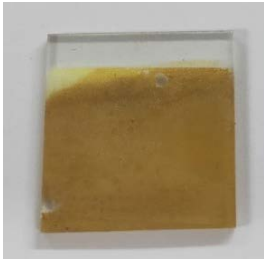
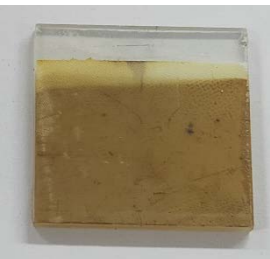
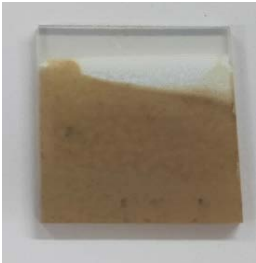
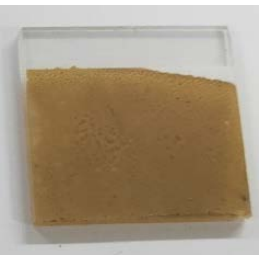
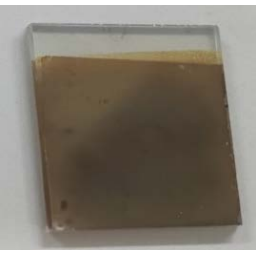
PDA adsorption at Au electrodes during CV oxidation of DA in aqueous solutions was investigated as functions of DA concentration, solution pH and potential-sweep rate with the use of electrochemical quartz crystal microbalance technique [14], in which two anodic peaks were observed at 0.19 and -0.25 V vs. SCE, designated as P_{a1} and P_{a2} respectively, and two cathodic peaks were observed at 0.09 and -0.31 V vs. SCE, designated as P_{c1} and P_{c2} respectively, in the phosphate buffer solution (pH = 7.4). Following reversible electrochemical reactions were attributed to these peaks;



where DA, DAQ, LDAC and DAC represent dopamine, dopamine quinone, leucodopaminechrome and dopaminechrome, respectively. It was concluded that the intramolecular cyclization of the first-step oxidation product of DA occurred significantly and further isomerization and oxidation of the cyclization product led to polymer growth at an Au electrode [14]. In the current work, the potentials of anodic peaks were much higher than those reported in Ref. [14], which would be due to the difference in the working electrode. The working electrode used in this work, TiO_2 coated on TCO, would require a much higher over-potential than Au electrode used in Ref. [14]. However, the fact that the PDA polymerization proceeded not at pH less than 5.0 but at pH higher than 7.0 was consistent with the current experimental results. It was reported that redox peaks shifted negatively with the increase of solution pH [14], which was also confirmed in the current experimental results. Consequently, the ECECEE (“E” denotes the electrochemical reactions while the “C” denotes the chemical reactions) mechanism for DA oxidation and subsequent polymerization for PDA formation [14] would be also applicable to the results obtained in this work. It was suggested that the presence of protons of relatively high concentration inhibited the coupled intramolecular cyclization of DAQ [14], which might be the cause for much less PDA formation at low pH in this work.

Table 1 summarizes the appearances of TiO_2 films and weight gain after electrochemical adsorption of PDA in an aqueous solution of pH 4.0, 6.0, 7.0 and 8.0 using THAM or MES as a buffer. It was found that the color of TiO_2 films after PDA adsorption became darker with increasing pH for both buffers. At low pH, brown color was deeper for THAM than for MES, and vice versa at high pH.

Table 1. Appearances of TiO₂ films and weight gain after electrochemical adsorption of PDA in aqueous solution of pH 4.0, 6.0, 7.0 and 8.0 using THAM or MES as a buffer.

pH	Buffer	THAM	MES
4.0	Appearance of TiO ₂ film		
	Weight gain	0.3 mg	0.3 mg
6.0	Appearance of TiO ₂ film		
	Weight gain	0.7 mg	0.4 mg
7.0	Appearance of TiO ₂ film		
	Weight gain	0.7 mg	0.5 mg
8.5	Appearance of TiO ₂ film		
	Weight gain	1.1 mg	0.7 mg

Weight gains after PDA adsorption increased with increasing pH, using THAM as buffer gave larger weight gains as expected from the CV curves. It is noteworthy that weight gains were smaller for MES than THAM, even though the color was deeper for MES, especially at pH 8.5. As mentioned earlier, the self-polymerization of DA molecules at high pH would give PDA a higher molecular weight that would result in longer π -conjugated systems with a high molar absorption coefficient.

Figure 6(a) and **Figure 6(b)** compare the I-V curves of PDA-coated DSSC using THAM and MES, respectively. At pH 4.0, using THAM and MES as buffer both produced certain levels of photocurrents closed to that produced by TiO₂ film without any dyes, which would be expected by the fact that almost no anodic currents in CV curves were observed and the colors of TiO₂ films were very pale at pH 4.0 for both buffers. At pH 6.0 and 7.0, using THAM as buffer gave higher photocurrent than that at pH 4.0 suggesting that PDA dye would possess the sensitized effect. However, using MES gave much fewer photocurrents than using THAM at pH 6.0 and 7.0, even though TiO₂ films were colored brown. At pH 8.5, almost no photocurrent was produced for both buffers, even though the colors of TiO₂ films were the darkest. As above discussed, negatively charged MES molecules would be attracted to the TiO₂ electrode to inhibit the adsorption of DA molecules on TiO₂ surface when the potential of working electrode was positively polarized, and the self-polymerized PDA in aqueous solution would be physically, not chemically, adsorbed on the TiO₂ surface. If PDA were not chemically adsorbed on the TiO₂ surface, excited electrons in PDA dye during irradiation would not be transferred to the conduction band of TiO₂ though the chemical bonding between them. This speculation would also be applied for the cases at pH 8.5 in both buffers. Physically adsorbed PDA on the TiO₂ surface would merely absorb incident light, which decreased the light intensity to decrease the number of photoelectrons in the TiO₂ conduction band resulting in much lower photocurrents without any dyes. The maximum η obtained in these experiments was calculated to be 0.049% at pH 7.0 using THAM, which would be extremely low as DSSC performance. It was reported that the zeta potential of DA-adsorbed TiO₂ particle was highly positive at pH higher than 7 and increased with DA concentration [12]. Since DA molecules in the aqueous solution were also positively charged at pH lower than 7, DA molecules

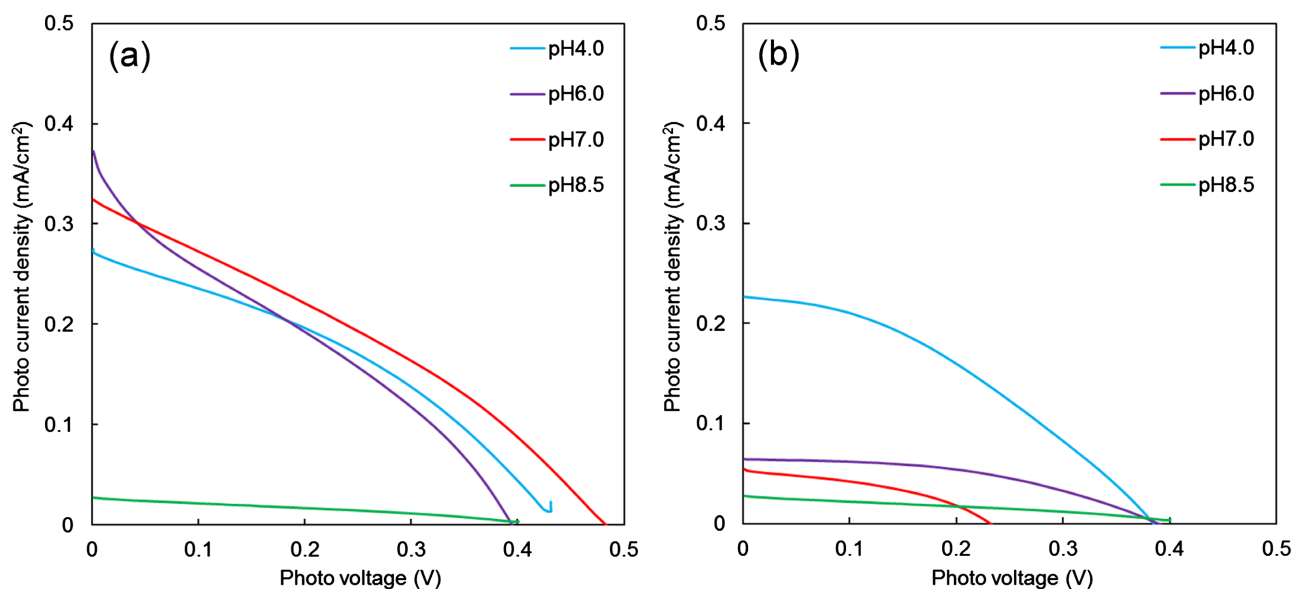


Figure 6. I-V curves of PDA-coated DSSC fabricated at pH 4.0, 6.0, 7.0 and 8.5 using (a) THAM and (b) MES as a buffer.

would repel against the surface of DA-adsorbed TiO₂ particles.

3.2. PDA Adsorption without Buffer

Experimental results obtained in the above section suggest that MES molecules would strongly adsorb on the surface of TiO₂ particles to inhibit the adsorption of DA molecules. Since a THAM molecule possesses one amino group and three hydroxyl groups, it might also inhibit the adsorption of DA molecules. Thus, electrochemical oxidation of DA without any buffer was investigated. **Figure 7(a)** shows the CV curves of DA obtained at pH 7.0 without buffer, which was found to be significantly different from those obtained with THAM and MES buffers at pH 7.0 as shown in **Figure 4(a)** and **Figure 4(b)**, respectively. Two cathodic peaks were clearly observed at about -0.05 and -0.35 V vs. Ag/AgCl, which were close to those observed at 0.09 and -0.31 V vs. SCE in the previous work [14]. Two anodic peaks at about 0.55 and 0.73 V vs. Ag/AgCl were observed from the second cycle onward, although only one anodic peak at about 0.55 V vs. Ag/AgCl was observed in the first cycle. These anodic peaks were also observed in **Figure 4** and **Figure 5(a)**. As discussed in the above section, the working electrode used in this work, TiO₂ coated on TCO, would require a much higher over-potential than Au for oxidation. Considering this influence, it would be concluded that over all CV-curves obtained in this work without buffer are quite similar to those reported in Ref. 14. **Figure 7(b)** shows the I-V curves of PDA-coated DSSC fabricated at pH 6.0, 7.0 and 8.5 without buffer. Compared with those shown in **Figure 6(a)**, both V_{oc} and I_{sc} are quite similar, however, the fill factor (FF) is much higher without buffer than that with THAM buffer, and η is calculated to be about 0.065%, which is much higher than the maximum η about 0.049% with THAM buffer. This suggests that THAM buffer adsorbed on

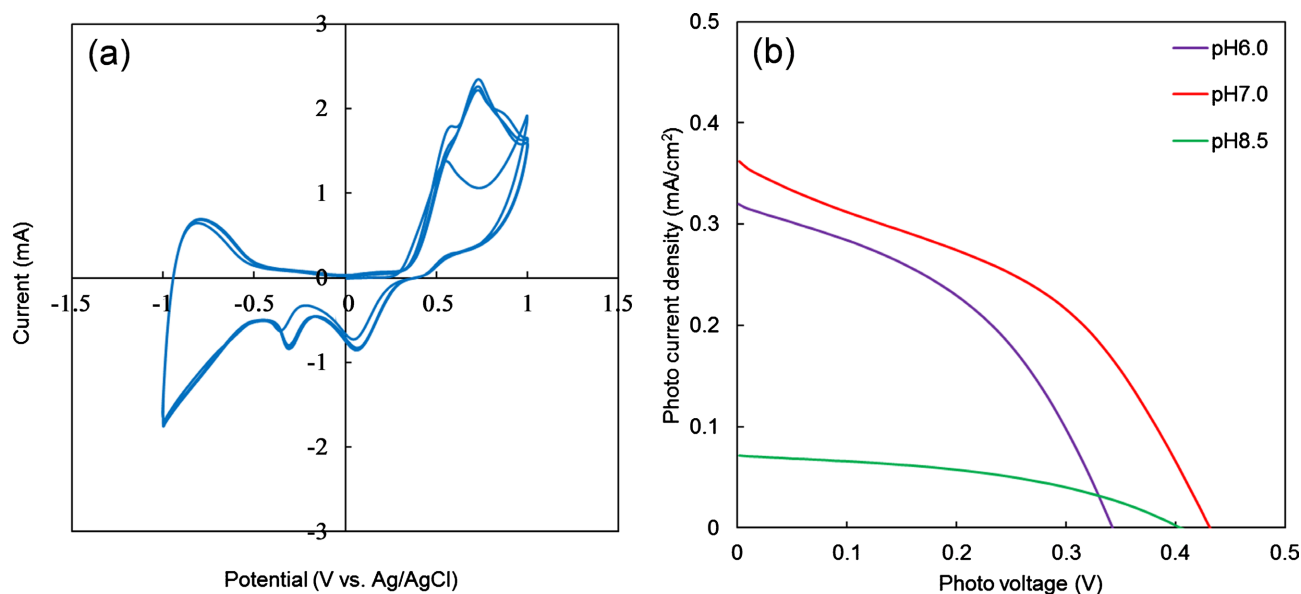


Figure 7. (a) Cyclic voltammograms of DA obtained at pH 7.0 without buffer; (b) I-V curves of PDA-coated DSSC fabricated at pH 6.0, 7.0 and 8.5 without a buffer.

the TiO₂ surface might inhibit the electrochemical oxidation of DA although THAM buffer was used for fabricating PDA (DC)-DSSC [10].

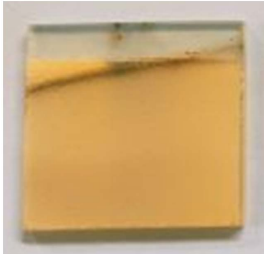
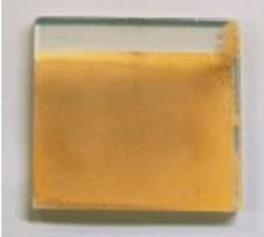

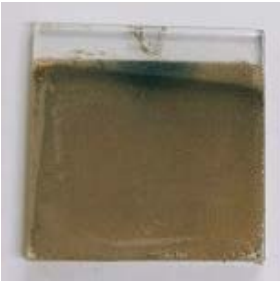
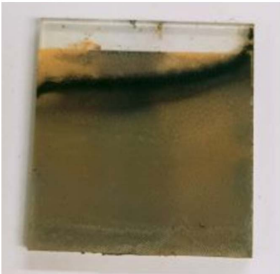
3.3. Effect of Adsorption Time and Electrode Potential

Because the adsorption time was only 30 min. in the preceding experiments, it was prolonged up to 8 hrs. **Table 2** summarizes the appearances of TiO₂ films and weight gain after electrochemical adsorption of PDA for 0.5, 1, 2, 4 and 8 hrs in aqueous solution at pH 7.0 without buffer. The brown color became darker with increasing adsorption time, and after 4 and 8 hrs, the film colors were dark brown. The weight gain after adsorption increased with increasing adsorption time, however, the amount of adsorbed PDA was only limited to 0.3% - 0.5% of the total amount of DA dissolved in aqueous solution.

Figure 8 shows the I-V curves of DSSCs after electrochemical adsorption of PDA in aqueous solution at pH 7.0 without buffer for 0.5, 1, 2, 4 and 8 hrs. It was found that I_{sc} did not change significantly up to 2 hrs and decreased after 4 hrs, however, V_{oc} monotonically decreased with increasing adsorption time yielding $\eta = 0.065\%$, 0.049% , 0.049% , 0.038% and 0.026% , respectively. This apparent contradiction would be due to the increased resistivity of PDA with a larger degree of polymerization. The addition of dopants that would decrease the resistivity of PDA might improve η .

As mentioned in the previous section, two cathodic peaks were clearly observed at about -0.05 and -0.35 V vs. Ag/AgCl in Fig. 7 (a), which may be attributed to the reduction of DAQ and DAC, the intramolecular cyclization reaction product of DAQ, respectively, according to the ECECEE mechanism [14]. Because PDA formation might be improved by suppressing these reverse reactions, electrode potential was fixed at $+1.0$ V vs. Ag/AgCl or potential sweep range was changed to $-0.5 - +1.0$ V vs. Ag/AgCl instead of $-1.0 - +1.0$ V vs. Ag/AgCl. **Figure 9** compares the I-V curves of DSSCs after electrochemical adsorption of PDA in aqueous solution at pH 7.0 without buffer for 30 min using the electrode potentials above mentioned. When the electrode potential was fixed at $+1.0$ V vs. Ag/AgCl, both V_{oc} and I_{sc} significantly decreased, which suggests that the reversal of electrode potential from positive to negative would be essential for the electrochemical adsorption of PDA. Since DA exists as a neutral molecule or DA⁺ ion in an aqueous solution at pH 7.0, DA⁺ ions would be attracted to a working electrode when the potential was negative, and then they would be oxidized when the electrode potential returned to positive. When the potential sweep range was changed to $-0.5 \sim +1.0$ V vs. Ag/AgCl instead of $-1.0 \sim +1.0$ V vs. Ag/AgCl, V_{oc} slightly decreased but I_{sc} slightly increased that improved η from 0.065% to 0.073% . This change of negative electrode potential would suppress the reverse reduction reactions of oxidized DA at positive electrode potential. This experiment would suggest the importance of optimization not only in electrode potential but also sweep rate. Further investigation would be necessary to improve η using the electrochemical adsorption of PDA.

Table 2. Appearances of TiO₂ films and weight gain after electrochemical adsorption of PDA for 0.5, 1, 2, 4 and 8 hrs in aqueous solution at pH 7.0 without a buffer.

Adsorption time 0.5 hr	Appearance of TiO ₂ film	
	Weight gain	0.6 mg
Adsorption time 1 hr	Appearance of TiO ₂ film	
	Weight gain	0.6 mg
Adsorption time 2 hr	Appearance of TiO ₂ film	
	Weight gain	0.8 mg
Adsorption time 4 hr	Appearance of TiO ₂ film	
	Weight gain	1.0 mg
Adsorption time 8 hr	Appearance of TiO ₂ film	
	Weight gain	1.1 mg

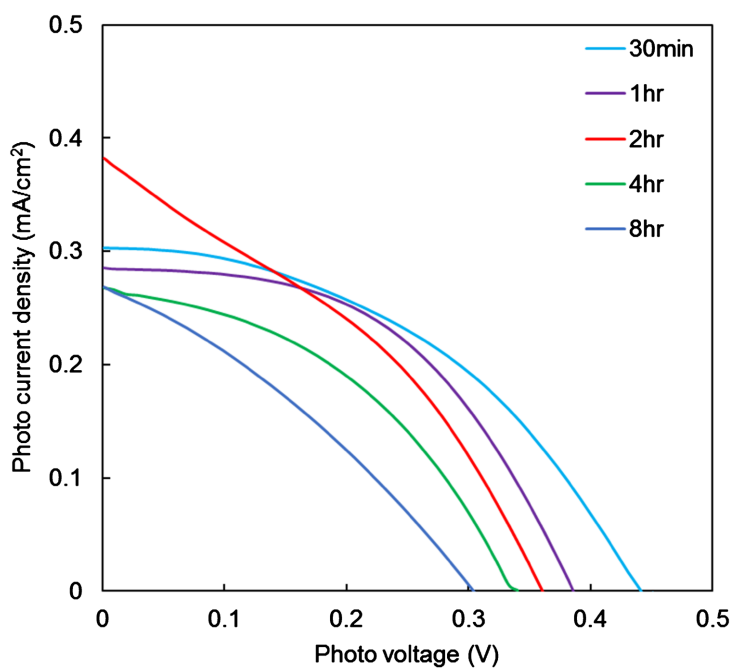


Figure 8. I-V curves of DSSCs after electrochemical adsorption of PDA in aqueous solution at pH 7.0 without a buffer for 0.5, 1, 2, 4 and 8 hrs.

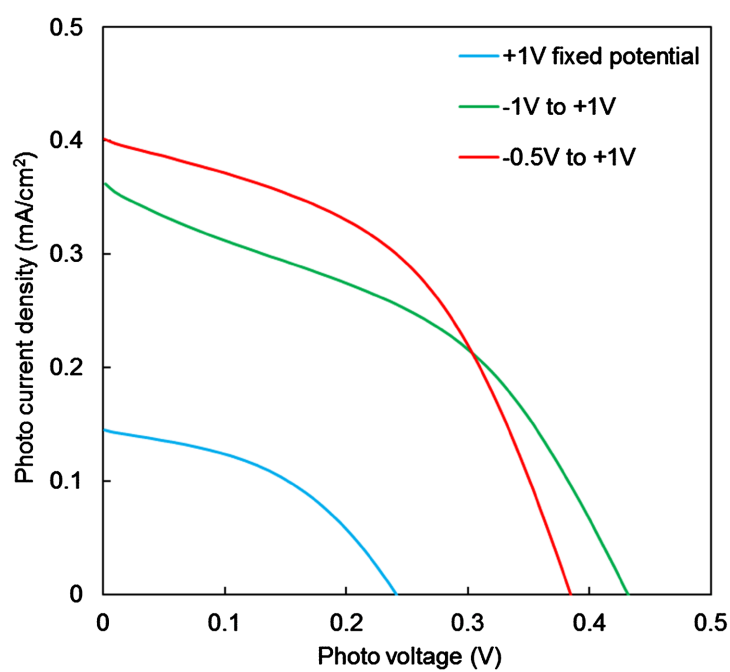


Figure 9. I-V curves of DSSCs after electrochemical adsorption of PDA in aqueous solution at pH 7.0 without a buffer for 30 min using fixed electrode potential at +1.0 V vs. Ag/AgCl, or potential sweep range of -0.5 ~ +1.0 V vs. Ag/AgCl, or potential sweep range of -1.0 ~ +1.0 V vs. Ag/AgCl.

4. Conclusion

To fabricate PDA (CV)-DSSC with improved η , the effects of pH, buffer, adsorption time and electrode potential for the electrochemical oxidation and po-

lymerization of DA on TiO₂ film were investigated. The optimum pH was around 7. It was found that the use of a buffer, especially MES, significantly deteriorate the electrochemical adsorption of PDA, and the highest η was obtained without buffer. With increasing adsorption time, the amount of adsorbed PDA increased but η decreased, suggesting the increased resistivity of PDA with a larger degree of polymerization. It was suggested that the reversal of electrode potential from positive to negative would be essential for the electrochemical adsorption of PDA. Because any attempts for increasing η other than the conditions for the electrochemical adsorption of PDA like increasing TiO₂ surface area by the sol-gel method or using LiI electrolyte were not examined, η values reported in this work were lower than those reported in the previous works. However, it would be concluded that fundamental understanding for the electrochemical adsorption of PDA has been deepened, and directions for increasing η using this method have been demonstrated for future research.

Conflicts of Interest

The authors declare no conflicts of interest regarding the publication of this paper.

References

- [1] Nazeeruddin, M.K., Baranoff, E. and Gratzel, M. (2011) Dye-Sensitized Solar Cells: A Brief Overview. *Solar Energy*, **85**, 1172-1178. <https://doi.org/10.1016/j.solener.2011.01.018>
- [2] Fang, Z., Eshbaugh, A.A. and Schanze, K.S. (2011) Low-Bandgap Donor-Acceptor Conjugated Polymer Sensitizers for Dye-Sensitized Solar Cells. *Journal of the American Chemical Society*, **133**, 3063-3069. <https://doi.org/10.1021/ja109926k>
- [3] Persson, P., Bergstro, R. and Lunell, S. (2000) Quantum Chemical Study of Photoinjection Processes in Dye-Sensitized TiO₂ Nanoparticles. *The Journal of Physical Chemistry B*, **104**, 10348-10351. <https://doi.org/10.1021/jp002550p>
- [4] Rajh, T., Chen, L.X., Lukas, K., Liu, T., Thurnauer, M.C. and Tiede, D.M. (2002) Surface Restructuring of Nanoparticles: An Efficient Route for Ligand-Metal Oxide Crosstalk. *The Journal of Physical Chemistry B*, **106**, 10543-10552. <https://doi.org/10.1021/jp021235v>
- [5] Tae, E.L., Lee, S.H., Lee, J.K., Yoo, S.S., Kang, E.J. and Yoon, K.B. (2005) A Strategy to Increase the Efficiency of the Dye-Sensitized TiO₂ Solar Cells Operated by Photoexcitation of Dye-to-TiO₂ Charge-Transfer Bands. *The Journal of Physical Chemistry B*, **109**, 47, 22513-22522. <https://doi.org/10.1021/jp0537411>
- [6] Dimitrijevic, N.M., Poluektov, O.G., Saponjic, Z.V. and Rajh, T. (2006) Complex and Charge Transfer between TiO₂ and Pyrroloquinoline Quinone. *The Journal of Physical Chemistry B*, **110**, 25392-25398. <https://doi.org/10.1021/jp064469d>
- [7] Lee, H., Dellatore, S.M., Miller, W.M. and Messersmith, P.B. (2007) Mussel-Inspired Surface Chemistry for Multifunctional Coatings. *Science*, **318**, 426-430. <https://doi.org/10.1126/science.1147241>
- [8] Lyu, Q., Song, H., Yakovlev, N.L., Tan, W.S. and Chai, C.L.L. (2018) *In Situ* Insights into the Nanoscale Deposition of 5,6-dihydroxyindole-Based Coatings and the Implications on the Underwater Adhesion Mechanism of Polydopamine Coatings. *RSC Advances*, **8**, 27695-27702. <https://doi.org/10.1039/C8RA04472D>

- [9] Liebscher, J. (2019) Chemistry of Polydopamine—Scope, Variation, and Limitation. *European Journal of Organic Chemistry*, **2019**, 4976-4994. <https://doi.org/10.1002/ejoc.201900445>
- [10] Nam, H.J., Kim, B., Ko, M.J., Jin, M., Kim, J.M. and Jung, D.-Y. (2012) A New Mussel-Inspired Polydopamine Sensitizer for Dye-Sensitized Solar Cells: Controlled Synthesis and Charge Transfer. *Chemistry—A European Journal*, **18**, 14000-14007. <https://doi.org/10.1002/chem.201202283>
- [11] Mozaffari, S., Nateghi, M.R. and Zarandi, M.B. (2014) Effects of Multi Anchoring Groups of Catecholamine Polymer Dyes on the Electrical Characteristics of Metal Free Dye-Sensitized Solar Cells: A Comparison Study. *Solar Energy*, **106**, 63-71. <https://doi.org/10.1016/j.solener.2013.11.030>
- [12] Sallem, F., Villatte, L., Geffroy, P.-M., Goglio, G. and Pagnoux, C. (2020) Surface Modification of Titania Nanoparticles by Catechol Derivative Molecules: Preparation of Concentrated Suspensions. *Colloids and Surfaces A: Physicochemical and Engineering Aspects*, **602**, 125167. <https://doi.org/10.1016/j.colsurfa.2020.125167>
- [13] Bahri, S., Jonsson, C.M., Jonsson, C.L., Azzolini, D., Sverjensky, D.A. and Hazen, R.M. (2011) Adsorption and Surface Complexation Study of L-DOPA on Rutile (α -TiO₂) in NaCl Solutions. *Environmental Science & Technology*, **45**, 3959-3966. <https://doi.org/10.1021/es1042832>
- [14] Li, Y., Liu, M., Xiang, C., Xie, Q. and Yao, S. (2006) Electrochemical Quartz Crystal Microbalance Study on Growth and Property of the Polymer Deposit at Gold Electrodes during Oxidation of Dopamine in Aqueous Solutions. *Thin Solid Films*, **497**, 270-278. <https://doi.org/10.1016/j.tsf.2005.10.048>